

RESEARCH ARTICLE

Tube Sheet Annular Seam Measurement Technology Based on Laser Collaboration With Vision Sensor

JIANHUA MA¹, XINGDONG WANG¹, JIANYI KONG¹, YOUMIN RONG², AND YU HUANG²¹Key Laboratory of Metallurgical Equipment and Control Technology, Wuhan University of Science and Technology, Wuhan 430080, China²State Key Laboratory of Digital Manufacturing Equipment and Technology, Huazhong University of Science and Technology, Wuhan 430080, China

Corresponding author: Xingdong Wang (wangxingdong@wust.edu.cn)

This work was supported in part by the Key Research and Development Program of Hubei Province, China, under Grant 2021BAA195.

ABSTRACT The fast and accurate locating of the tube-sheet annular seam is the key factors to ensure the high efficiency and quality of automatic welding of pressure vessels. Considering the problems of welding sheet deformation and tubes deviation caused by machining process and welding thermal, this paper builds an automatic welding robot platform, which is equipped with a measurement system coordinated by multiple lasers and visual sensors, and put forward a real-time welding distance measurement method based on cross lasers and visual sensors, at the same time, the multi spot laser assisted vision sensor is used to quickly and accurately measure the center of the tube, so as to guide the adjustment of the welding robot and posture of the welding torch in real time. Then, through the measurements of system error, static and dynamic measurement error, it is known that the dynamic accuracy of tube sheet welding distance is not less than 0.22mm, and the positioning accuracy of welded tube center is not less than 0.219mm, which can meet the accuracy requirements of automatic tube sheet welding.

INDEX TERMS Machine vision, laser, annular welds, tube-sheet welding.

I. INTRODUCTION

Pressure vessels play an important role in many industries related to the national economy and people's livelihood, such as petrochemicals, nuclear power ships, metallurgical and military industries [1], [2]. Pressure vessels such as tube-sheet heat exchangers (as shown in the Fig. 1), condensers, and steam generators are the main industrial products for heat exchange [3]. The welding quality of the container can easily lead to disasters such as combustion, fire, leakage and explosion, which not only endanger the safety of life and property, but also cause serious environmental pollution accidents.

The processing and manufacturing of pressure vessels is still dominated by manual arc welding or special welding machines. The appearance of the welding seam is not beautiful, and the quality is difficult to guarantee stability and consistently [4]. Compared with manual arc welding, the production efficiency and welding quality of special tube

sheet welding machines have a certain degree. However, for the locating of the welding position of the annular weld, that is, the distance between the tungsten and the outer wall of the tube, the tungsten and the tube sheet, the special tube sheet welding machine still relies on manual positioning of the annular seam one by one, and the consistency of welding quality is difficult to guarantee [5]. Moreover, it is difficult for the special tube-sheet welding machine to adapt to the thermal deformation of tube-sheet welding, and the welding process requires manual observation and intervention throughout the process, resulting in a harsh working environment and high labor intensity [6]. Therefore, it is an important technical means to ensure the welding quality to use a suitable detection method to locate the weld position before welding [7].

Many scholars have carried out contact and non-contact research work on the location of tube sheet welds before welding. In contact measurement, sensors such as electrical signals and displacements are arranged at the end of tungsten [8], and the welded tube is contact scanned, and then the position of the center of the tube is calculated by


The associate editor coordinating the review of this manuscript and approving it for publication was Ravibabu Mulaveesala .



FIGURE 1. The tube-sheet heat exchangers.

fitting. This method has high measurement accuracy, but the measurement speed is slow and there is contact safety. The non-contact measurement is mainly based on the visual measurement method, which has the advantages of no contact between the visual information and the work-piece, a large amount of information, high sensitivity and precision, and anti-electromagnetic interference [9]. It is divided into passive vision [10] and active vision [11], according to additional lights. Passive vision mainly uses arc light or natural light generated by welding as the light source [12]. Active vision sensing mainly illuminates the work-piece through light sources such as ring light, spot light, and linear structured light, and collects the reflected structured light through a camera to obtain image information [13]. Some scholars use the crossline structured light mark to assist the visual acquisition of the line structured light and the feature points of the tube wall to calculate the position of the center of the tube. Some scholars also use red light as the active light source. After the camera obtains the image of the round tube, the center of the tube is calculated by the method of edge feature extraction. However, due to the process requirements of double layer welding of tube-sheet welding, when the tube is welded once, the tube will turn black, which interferes with the visual measurement during the second layer welding, resulting in a decrease in the accuracy of the circle center recognition.

Lasers are widely used in mechanical manufacturing and measurement fields because of their advantages of good straightness, strong anti-interference ability, and non-contact detection, and are suitable for vision sensors. Laser vision sensors can be divided into: single line laser [14], [15], cross line laser [16], [17], multi-line laser [18], spot laser [19], grid line laser, etc. Some scholars use a unique ring laser vision sensor to identify the weld seam of the work-piece. According to the image characteristics of the ring laser, the collected images are processed by denoising, segmentation, and refinement to obtain the weld seam characteristics and then realize the weld seam through template matching [20]. For tube-sheet annular welds, some scholars proposed to use cross lasers as an additional light source, and calculate the center position of the tube through the four feature points of the tube, so as to guide the robot to locate the center of the tube [21]. In this paper, a welding distance measurement method based on cross laser and vision sensor is proposed. At the same time, a method for measuring the center position

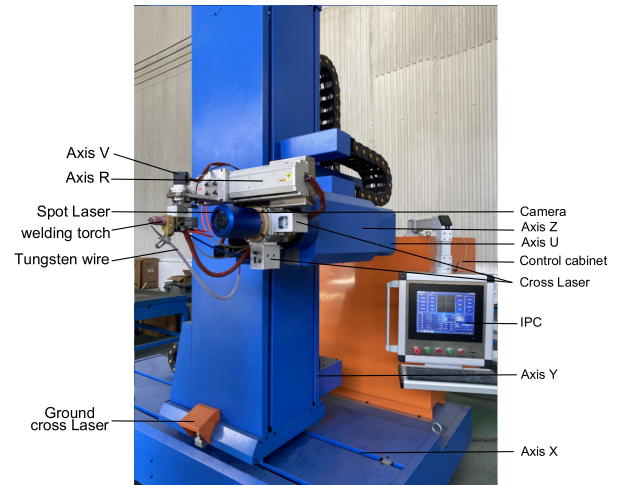


FIGURE 2. Tube-sheet welding robot.

of the welded tube based on the area laser formed by six spot lasers and the vision sensor is proposed, and several experiments are carried out through the actual tube sheet welding process. Therefore, the proposed measurement system has the following advantages: 1. It does not rely on manual instruction; 2. The low efficiency contact measurement method is abandoned, and the online measurement method of laser light source and vision collaboration is proposed, which not only meets the requirements of accuracy, but also greatly improves the efficiency; 3. Laser light is introduced for advantages of good straightness, strong anti-interference ability, and non-contact detection, and it is more stable and reliable than ordinary light source and greatly improve the stability of the measurement system.

II. TUBE-SHEET WELDING ROBOT

The experimental platform consists of a coordinate robot, TIG (tungsten inert gas) welding machine, cross laser and spot laser, CMOS camera and welding torch components, as shown in Fig.2. The U-axis rotation controls the welding torch to realize the circular seam welding, the movement of the XY-axis are used to locate the center of the welded tube, the Z-axis adjusts the welding distance from the welding torch to the sheet, and the V-axis and R-axis respectively control the welding inclination angle and welding radius of the welding torch, W-axis is used to automatically feed tungsten wire, and the other ABC-axis can be automatically adjusted to adapt to the work-piece.

The work-piece is a tube sheet (material Q345R) whose diameter and thickness are 950mm and 40mm, respectively, the inner dimensions of the tube is 19 mm and 2.5 mm wall thickness. The welding torch and the sheet are respectively connected to the positive and negative poles of the TIG welding machine.

The CMOS camera (Daheng MER2-503-23GM-P) is co-axial with the U-axis rotation center, and the synchronous rotation with the welding torch is realized through the optical fiber slip ring. At the same time, the water-air slip ring

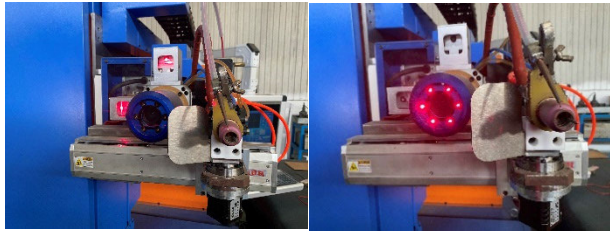


FIGURE 3. Cross laser and spot laser.

TABLE 1. Parameters of cross laser and spot laser.

Parameter	Cross Laser	Spot Laser
Wavelength	650±5nm	650±5nm
Output Power	≤100.0mW	≤100.0mW
Operating voltage	5.0VDC	5.0VDC
Laser mode	Pulse	Continuous Wave
Line Width/ Beam Size	≤20um (220mm)	R=20mm(220mm)
Parameter	Cross Laser	Spot Laser

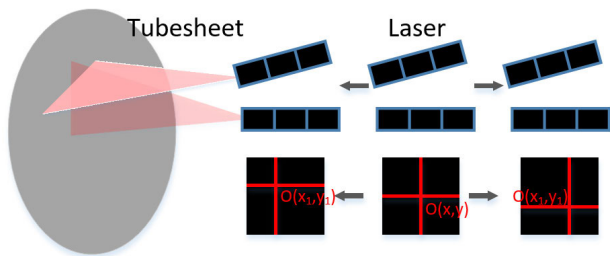


FIGURE 4. Cross laser and work piece image.

realizes the water cooling and argon protection device. The distance from the welding torch to the sheet is measured by a cross laser and a CMOS camera, but the measurement accuracy can only be guaranteed when the camera and the sheet are within a certain range. The cross laser is formed by two single line laser projections. The X projection laser is installed directly above the camera, and the Y projection laser is installed on the right side of the camera at 90 degrees to the X projection laser, as shown in Fig. 3. The cross laser parameters are shown in the table 1. The measurement of the center of the welded tube is measured by spot lasers and a CMOS camera, and it must be taken at a suitable position to obtain higher measurement accuracy. Because a single spot laser provides 20mm circle illumination, we assemble six spot lasers to increase the area to 55mm. Through calculated the physical angle, we design a special part to assemble the six spot lasers to ensure that the error was within a reasonable range, as shown in Fig. 3. They can meet the identification of the welded tube in the range of 20mm-55mm. The parameters of the circular spot laser are shown in Table 1. Because the power of lasers is very low and only turned on for a short time, the thermal effect can be ignored.

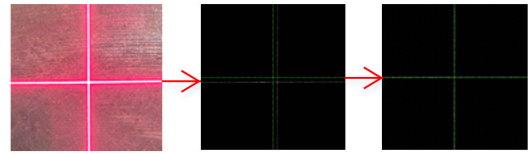


FIGURE 5. Calibration of cross laser.

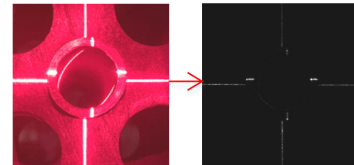


FIGURE 6. Cross laser image of tube sheet.

III. CALIBRATION OF CROSS LASER VISION SYSTEM

The principle of cross laser ranging: two orthogonal lines of laser throw on the surface of the tube sheet at a certain angle, and then the CMOS camera obtains the front cross laser stripe image of the tube sheet as shown in Fig. 4. When the distance between the tube sheet and the welding torch changes (the thermal deformation of the tube sheet), the focus position of the image cross laser stripes will move regularly, that is, there is a specific relationship between the degree of deformation of the tube sheet and the degree of change of the intersection point.

A. CALIBRATION OF CROSS LASER VISION SYSTEM

Firstly, the distance between the work-piece and the camera is adjusted to 220mm by the tube sheet welding robot, and the horizontal line laser and vertical line laser throw on the tube sheet at the same time, and then the inclination and relative position of the cross laser are adjusted to make the fringe of cross laser fringe coincides with the image coordinate axis. The process of calibration is shown in Fig. 5, which is used as the reference position for the camera to obtain the image, and the actual length in the XY direction corresponding to a single pixel is calculated according to the number of image pixels and the actual shooting range. In all the tests in this paper, the position of photographing is the calibration position, including the calculation of welding distance deviation and annular seam center deviation.

B. SAMPLE AND ANALYSIS OF CROSS LASER IMAGE

Move the camera to the above-mentioned reference position for taking pictures by the tube sheet welding robot (the distance between the camera and the tube-sheet is about 220mm), and then adjust the robot to take the picture roughly to the welded tube, so that the cross laser throw on the center of the tube, actual projection and imaging are shown in Fig. 6.

1) IMAGE PREPROCESSING

Since the welded tube is convex relative to the sheet, the single line laser image is divided into 7 sections, as shown in Fig. 7, the first and seventh sections are the welding sheet

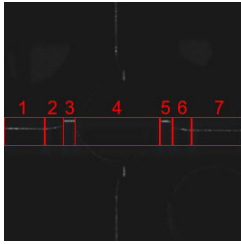


FIGURE 7. Segment of tube image.

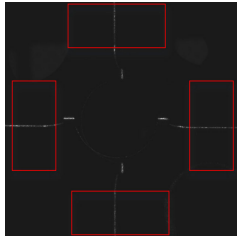


FIGURE 8. Cross laser image segmentation.

imaging area, the second and sixth sections are the welding seam imaging area, and the third and fifth sections are the imaging area of the tube wall, and section 4 is the imaging area inside the tube. Therefore, in order to measure the welding distance from the welding torch to the annular seam of the tube sheet, the imaging area data of sections 1 and 7 should be used as the criterion, and other interference areas should be excluded.

In order to improve the detection accuracy, the straight-line equation of the cross laser is accurately calculated, and the first and seventh segments of the single line laser are selected to characterize the imaging state of the line laser, as shown in Fig. 8, to obtain the equation of the single line laser line.

2) LINEAR FITTING AND INTERSECTION COORDINATE CALCULATION OF THE LINE LASER

Since the line laser imaging is still a straight-line feature, a straight line can be fitted according to the feature centroid coordinate points extracted above. The initial throw image of the cross laser is a straight line in the horizontal and vertical directions, and the acquired image is still a straight line in the horizontal and vertical directions. The vertical laser line equation can be expressed as:

$$x = az \tag{1}$$

The horizontal laser line equation can be expressed as:

$$y = bz \tag{2}$$

Therefore, the coordinates of the intersection point are (a, b) .

In order to calculate the straight-line equation of the cross laser, the gray value summation is performed on the rows and columns of the image respectively. The gray value summation

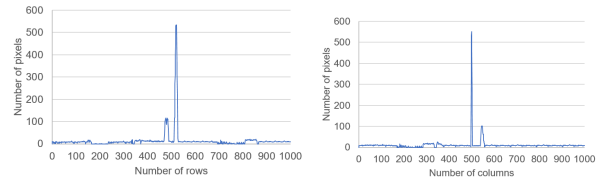


FIGURE 9. Gray value distribution of image rows and column.

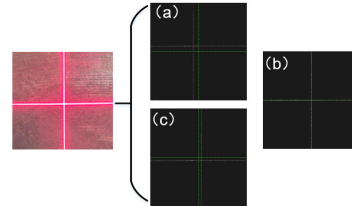


FIGURE 10. Cross laser stripe imaging.

TABLE 2. The relationship between X/Y deviation and Z coordinate.

Z	d_x	d_y	Z	d_x	d_y
218.0	-8	-3	220.0	0	1
218.4	-6	-2	220.4	1	3
218.8	-5	-1	220.8	2	3
219.2	-3	0	221.2	4	4
219.6	-2	0	221.6	6	5

formulas of the row and the column are shown in (3) and (4):

$$G(r) = \sum_{x=1}^n g(x, r) \tag{3}$$

$$G(c) = \sum_{y=1}^m g(c, y) \tag{4}$$

In the formula, $G(r)$ and $G(c)$ are the sum of the gray values of the row and column, respectively, m and n are the number of rows and columns of image pixels, respectively, and $g(x, y)$ represents the pixel point (x, y) gray value, the image gray value distribution is shown in Fig. 9.

It can be seen that the values of a and b can be obtained through the proportional relationship between the row and the column corresponding to the work-piece coordinate system.

C. MATHEMATICAL MODEL OF AXIAL WELD DISTANCE AND CROSS POINT LOCATION

The large amount of welding heat generated during the welding process may cause the deformation of the tube sheet. In order to ensure the welding quality, the welding distance needs to be re-measured and positioned before each tube welding. Therefore, it is necessary to calculate the welding distance through the cross laser and adjust the distance between the welding torch and the sheet in real time.

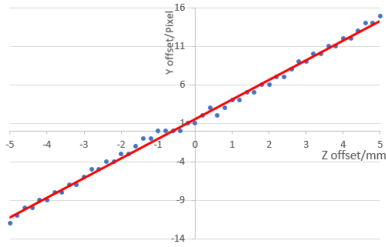


FIGURE 11. X pixel offset value and Z offset coordinate.

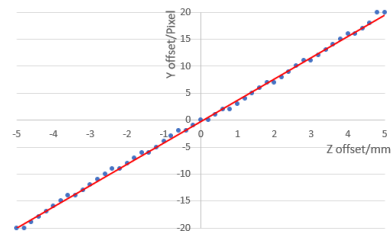


FIGURE 12. Y pixel offset value and Z offset coordinate.

1) SIMULATION TEST OF AXIAL THERMAL DEFORMATION

The axial thermal deformation simulation process is: adjust the camera to the photographing position ($Z=220\text{mm}$) through the welding robot, and the cross laser is facing the sheet, as shown in the Fig. 10((a) and (c) are the near or far images of standard (b) respectively), the cross laser imaging coinciding with the XY coordinate axes, the Z direction is gradually move advance 5 times in units of 0.4mm, and the cross laser images are obtained respectively, and the deviation pixel of X and Y are calculated; after the Z direction returns to the original photographing position, gradually move back 5 times in units of 0.4mm to obtain cross laser stripe images respectively, as shown in Figure 10, and calculate the deviation pixel of X and Y. The test data are shown in Table 2. The distance of advancing and back can be regarded as the value of the axial thermal deformation of tube sheet welding. By analyzing the deformation amount and the deviation value of the cross-laser stripe, there is a certain relationship between the two.

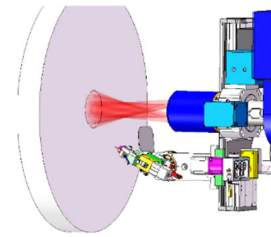


FIGURE 13. Image of tube-sheet.

2) MATHEMATICAL MODEL OF WELDING DISTANCE AND SINGLE LINE LASER, AND CALCULATION OF INTERSECTION COORDINATES

It can be seen from the above-mentioned cross laser ranging principle and preliminary test that there is a linear relationship between the welding distance and the XY deviation pixel. In order to establish a precise mathematical relationship, 50 positioning tests were carried out. The offset pixel in the XY direction is 0 (there are systematic errors $\varepsilon_X = 0, \varepsilon_Y = 1$), and d_Z is the measurement range of $\pm 5\text{mm}$ (it is assumed that the deformation of the welded tube does not exceed $\pm 5\text{mm}$), and the offset pixel in the XY direction in this range are d_X and d_Y , respectively.

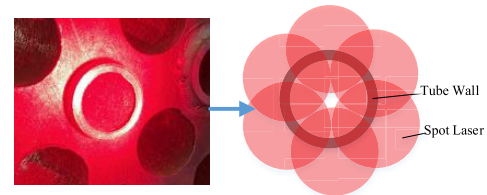


FIGURE 14. Schematic diagram of spot laser and work-piece imaging.

Suppose the linear equation is:

$$y = a + bx \tag{5}$$

The sum of squares of the deviations is:

$$\varepsilon = \sum_{i=1}^n (y_i - (a + bx_i))^2 = \sum_{i=1}^n (y_i - a - bx_i)^2 \tag{6}$$

To minimize ε , according to the principle of least squares:

$$a = \frac{\sum_{i=1}^n x_i y_i - \sum_{i=1}^n y_i \sum_{i=1}^n x_i}{(\sum_{i=1}^n x_i)^2 - n \sum_{i=1}^n x_i^2} \tag{7}$$

$$b = \frac{\sum_{i=1}^n x_i \sum_{i=1}^n y_i - n \sum_{i=1}^n x_i y_i}{(\sum_{i=1}^n x_i)^2 - n \sum_{i=1}^n x_i^2} \tag{8}$$

From the above formula, the straight-line equation of the deviation distance in the X direction and the change of the Z coordinate is:

$$x = 3.95z - 0.27 \tag{9}$$

The R-square value of the above formula is 0.9987, which meets the fitting requirements. The original data and the fitted straight line are shown in Fig. 11.

The equation of the straight line between the deviation distance in the Y direction and the change in the Z coordinate is:

$$y = 2.55z + 1.55 \tag{10}$$

The R-square value of the above formula is 0.9963, which meets the fitting requirements. The original data and the fitted straight line are shown in Fig. 12.

From the above offset rules of X and Y, it can be known that the coordinate value of the intersection point of the cross laser is:

$$(x, y) = (3.95z - 0.27, 2.55z + 1.55) \tag{11}$$

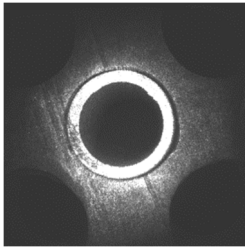


FIGURE 15. Image of spot laser and welded tube.

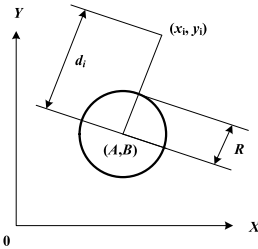


FIGURE 16. Least squares fit circle.

IV. ANNULAR SEAM MEASUREMENT BASED ON MULTI-SPOT LASER AND VISION SENSOR

In order to obtain more accurate circumferential seam feature data through vision and improve the anti-interference ability and accuracy of annular seam detection, the laser throw area formed by 6 spot lasers evenly covers the welded tube and its periphery, as shown in Figures 13 and 14. Sufficient energy is provided to separate areas such as the inside of the tube, the tube wall, and the sheet, which is convenient for image segmentation and information processing.

A. COLLECTION AND PREPROCESSING OF TUBE-SHEET ANNULAR SEAM IMAGE

The prior CAD drawing can guide the welding robot to align the camera center almost directly to the center of the welded tube. Due to the small deviation of thermal deformation or machining errors, it can be guaranteed that there is a complete annular seam in the acquired image. Moreover, the reference value of the inner diameter of the welded tube is known, and the circle information to be extracted during the image recognition process will refer to this value within a deviation range of no more than 20%. The image obtained by CMOS camera of the tube sheet is processed into a gray image. Since the grayscale steps in the tube, the wall and the outside of the tube is obvious, the image can be divided into three parts, as shown in Figure 15. However, by observing the image features, it can be seen that the outer area of the tube includes the gap between the tube and sheet, the annular weld pool, the sheet and other parts, and the information is relatively complex. But the inner circle of the tube can be fitted by extracting the image information in the tube and the tube wall.

B. FITTING OF INNER CIRCLE OF TUBE

During the processing of the welded tube, there may be damage to the inner wall, which may lead to the loss of

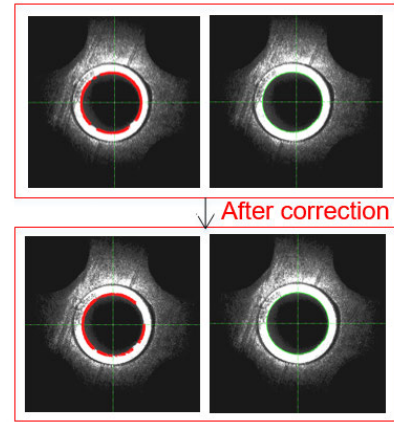


FIGURE 17. Fitting results.

the circular information, and at the same time, the welded tube may be thermally deformed due to welding heat. The position of the center of the circle is corrected, as shown in Figure 16.

The defining equation for the circle is shown:

$$(x - A)^2 + (y - B)^2 = R^2 \tag{12}$$

Let: $a = -2A$, $b = -2B$, $c = A^2 + B^2 - R^2$, then the circle equation becomes a linear equation with parameters (a, b, c) :

$$x^2 + y^2 + ax + by + c = 0 \tag{13}$$

Just calculate a, b, c , and it can be converted into 3 parameters of the circle:

$$\begin{cases} A = -\frac{a}{2} \\ B = -\frac{b}{2} \end{cases} \tag{14}$$

$$R = \frac{1}{2}\sqrt{a^2 + b^2 - 4c} \tag{15}$$

Given the set of boundary points (X_i, Y_i) , $i \in (1, 2, \dots, N)$, the distance d_i from each point to the center of the circle:

$$d_i^2 = (X_i - A)^2 + (Y_i - B)^2 \tag{16}$$

The square of the difference from the square of the radius of the circle is defined as:

$$\begin{aligned} \sum \delta_i^2 &= \sum (d_i^2 - R^2)^2 \\ &= \sum (X_i^2 + Y_i^2 + aX_i + bY_i + c)^2 \end{aligned} \tag{17}$$

According to the extreme value principle, when the function takes the minimum value, its derivative is zero, then:

$$\begin{cases} \frac{\partial(\sum \delta_i^2)}{\partial a} = \sum 2(X_i^2 + Y_i^2 + aX_i + bY_i + c)X_i = 0 \\ \frac{\partial(\sum \delta_i^2)}{\partial b} = \sum 2(X_i^2 + Y_i^2 + aX_i + bY_i + c)Y_i = 0 \\ \frac{\partial(\sum \delta_i^2)}{\partial c} = \sum 2(X_i^2 + Y_i^2 + aX_i + bY_i + c) = 0 \end{cases} \tag{18}$$



FIGURE 18. Tube-sheet with grooves.

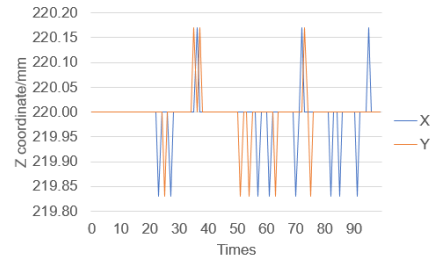


FIGURE 21. 100 times of welding distance static test data.

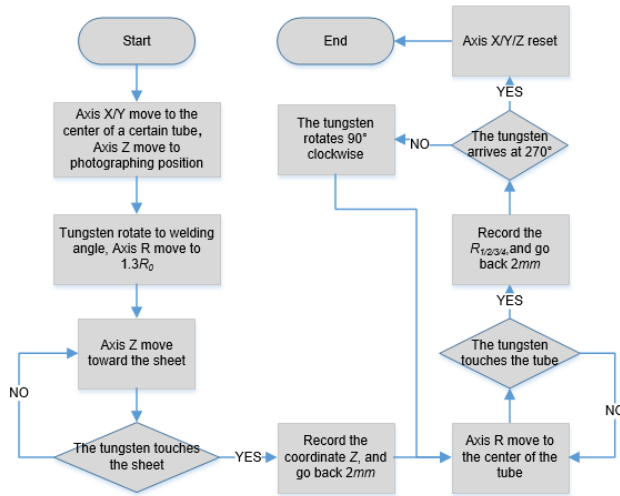


FIGURE 19. Tube sheet touching process.

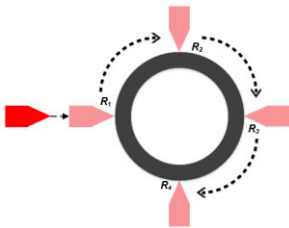


FIGURE 20. Schematic diagram of tube touch.

Solve this system of equations and let:

$$\begin{cases} C = N \sum X_i^2 - \sum X_i \sum X_i \\ D = N \sum X_i Y_i - \sum X_i \sum Y_i \\ E = N \sum X_i^3 - N \sum X_i Y_i^2 - \sum (X_i^2 + Y_i^2) \sum X_i \\ G = N \sum Y_i^2 - \sum Y_i \sum Y_i \\ H = N \sum Y_i^3 + N \sum X_i^2 Y_i - \sum (X_i^2 + Y_i^2) \sum Y_i \end{cases} \quad (19)$$

Available:

$$\begin{cases} a = \frac{HD-EG}{CG-D^2} \\ b = \frac{HC-ED}{D^2-GC} \\ c = -\frac{\sum (X_i^2 + Y_i^2) + a \sum X_i + b \sum Y_i}{N} \end{cases} \quad (20)$$

After obtaining a , b , and c , the fitted circular mathematical equation can be obtained.

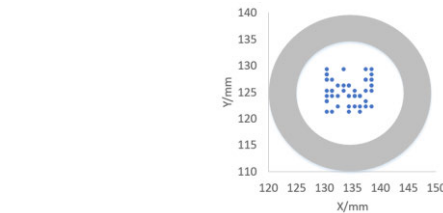


FIGURE 22. Sample points.

C. CALCULATE THE CENTER OF THE ANNULAR SEAM

In this working environment, the length corresponding to each pixel is 0.0548mm obtained through camera calibration. The circle fitted by the above least squares method is shown in Fig. 17, and its mathematical equation is:

Then the coordinates of the center of the circle are $(-\frac{a}{2}, -\frac{b}{2})$.

V. TEST AND ANALYSIS OF POSITIONING OF TUBE-SHEET ANNULAR SEAM

In actual tube sheet welding, there will be horizontal, vertical or cross-shaped tube sheet grooves, as shown in Fig. 18. The groove will affect the cross-laser measurement. Therefore, when there is a tube sheet groove, the calculation and measurement of welding distance is mainly based on unidirectional laser measurement, and the position of the groove is preset before the measurement.

A. TOUCH MEASUREMENT OF TUBE SHEET

The measurement method proposed in this paper is non-contact measurement, which has the advantages of high measurement efficiency and no contact with the work-piece. In order to verify the accuracy and stability of the data, the contact measurement data with high measurement accuracy is used as a standard reference. The measurement process is shown in the Fig.19 and Fig.20.

Assume that the initial angle of the U-axis is θ , the compensation value of X and Y are calculated as follows.

$$\begin{bmatrix} \Delta x \\ \Delta y \end{bmatrix} = \begin{bmatrix} \cos \theta & \sin \theta \\ -\sin \theta & \cos \theta \end{bmatrix} \begin{bmatrix} R_3 - R_1 \\ R_4 - R_2 \end{bmatrix} \quad (21)$$

B. TEST AND ANALYSIS OF WELDING DISTANCE MEASUREMENT OF TUBE-SHEET ANNULAR SEAM

It can be obtained from the formula (9) and (10) that the relationship between the welding distance z and the pixel

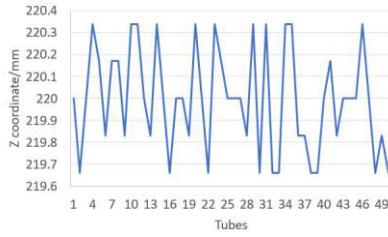


FIGURE 23. The measured date Z.

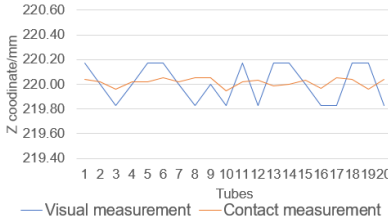


FIGURE 24. 20 times of welding distance dynamic test data.

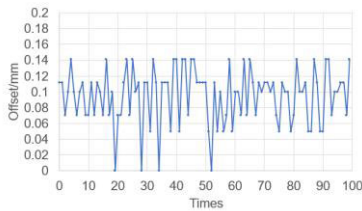


FIGURE 25. Offset of visual and contact measurement.

deviation in the X/Y direction is:

$$z = \frac{x + 0.27}{3.95 * 6} \tag{22}$$

$$z = \frac{y + 1.55}{2.55 * 6} \tag{23}$$

1) SYSTEM ERROR

In order to verify the stability of cross laser and visual measurement, 100 times of welding distance measurements were performed on randomly selected welded tubes (taking a single-layer welded tube as an example), and the measurement data are shown in Fig.21 below.

The actual distance between the welding torch and the welding sheet can be accurately measured by touching the welding sheet (as Fig.19), and the measurement data is = 220.00mm.

The system detection average error is:

$$\epsilon_x = \frac{\sum_{n=1}^{50} |z_{nx} - z_0|}{50} = 0.0187 \tag{24}$$

$$\epsilon_y = \frac{\sum_{n=1}^{50} |z_{ny} - z_0|}{50} = 0.0136 \tag{25}$$

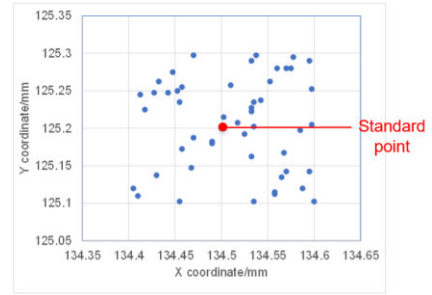


FIGURE 26. Static measurement data of 50 times.

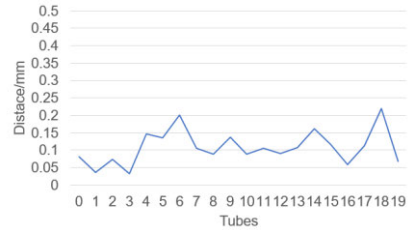


FIGURE 27. Dynamic measurement data of 20 tubes.

2) STATIC MEASUREMENT

There will be a slight deviation in the photographing position which is the rough positioning center, as the processing quality and thermal deformation change the position of the welded tube. So it is necessary to conduct a distance measurement test on the photographing points near the center of the tube. In this experiment, the distance of the same welded tube is measured within 20% of the deviation range of the center position radius, as shown in the Fig.22. Cross laser measurement data are shown in the Fig.23. From the measurement data, the accuracy of visual measurement and contact measurement within the deviation range of the center position of welded tube is more than 98%, and the maximum deviation is not more than 0.34mm. Therefore, visual measurement can be used instead of contact measurement.

The static detection average error is:

$$\epsilon = \frac{\sum_{n=1}^{50} |z_n - z_0|}{50} = 0.19 \tag{26}$$

3) DYNAMIC MEASUREMENT

The pressure vessel is usually composed of multiple welded tubes. In order to verify that the method is suitable for dynamic measurement, 20 different tubes were continuously measured, and contact measurement is carried out synchronously for each tube.

The measurement data is shown in Fig. 24.

Dynamic detection average error:

$$\epsilon_{max} = 0.22 \tag{27}$$

C. TEST AND ANALYSIS OF THE CENTER POSITIONING OF THE ANNULAR SEAM

Refer to the welding distance measurement, the center positioning of the annular seam takes the contact measurement (as Fig.19 and Fig.20) as the standard data.

TABLE 3. The error of welding distance and annular center.

	Welding distance (mm)	Annular Center (mm)
System error	0.018(average)	0.096(average)
Static error	0.19(average)	0.078(average)
Dynamic error	0.22(max)	0.219(max)

1) SYSTEM ERROR

In order to verify the accuracy and stability of the laser vision measurement of the annular seam, the random tube was measured and the data of the circle center was calculated. 100 times measurement data are shown in Fig. 25. The distance between visual data and contact data is less than 0.14mm.

The static detection average error is:

$$\epsilon_d = \frac{\sum_{n=1}^{100} \sqrt{(\Delta x^2 + \Delta y^2)}}{100} = 0.096 \quad (28)$$

2) STATIC MEASUREMENT

Similarly, due to the change of the center position caused by during processing and welding deformation, it is necessary to conduct many visual measurements of the center at the same tube, within 20% diameter of the roughly positioned center, and at the same time, we carry out contact measurement. The comparison of 50 measurement data is shown in the Fig.26. It can be seen from the data that the accuracy of the visual measurement and contact measurement of the center of the annular is more than 95%, and the maximum deviation is not more than 0.139mm, Therefore, visual measurement method can be used instead of contact measurement.

$$\delta_d = \frac{\sum_{n=1}^{100} \sqrt{(\Delta x^2 + \Delta y^2)}}{100} = 0.078 \quad (29)$$

3) DYNAMIC MEASUREMENT

In order to verify that the method is suitable for dynamic measurement, 20 tubes were continuously measured, and contact measurement is carried out synchronously for each tube. The measurement data is shown in the Fig.27.

Dynamic detection average error is:

$$\epsilon_{max} = 0.219 \quad (30)$$

D. ANALYSIS OF MEASUREMENT DATA

The error sources of the measurement system are camera resolution and mechanical repeated positioning accuracy, among which the camera resolution is the main factor. The camera selected by the measurement system is 5 million pixels, and the accuracy of a single pixel can be calculated as 0.0548mm according to the XY photo area, so the identification error of the annular seam center is great than 0.0548mm. The XYZ motor (Maxsine) equipped a 23-bit absolute encoder

is selected, to ensure that the repeated positioning error of the mechanical components is less than 0.05mm. Therefore, the camera measurement accuracy is lower than other factors. According to the Z direction measurement law, a single pixel moves 0.17mm in the Z-direction, and the deviation is larger than that the XY direction. However, the welding distance is obtained by cross laser vision calculation, so the interference factors are not as complex as the annular seam image, so the calculation accuracy is higher than the annular seam center.

The collaborative measurement system is based on laser and visual sensor. The system deviation, static and dynamic measurement deviation data are shown in Table 3. In particular, the maximum dynamic measurement deviation is 0.22mm and 0.219mm respectively, which can fully meet the measurement accuracy of tube sheet welding. Therefore, the efficient visual measurement method can be used instead of the contact measurement method, and its measurement data can accurately characterize the tube sheet annular seam.

VI. CONCLUSION

This paper mainly proposes the measurement method of the axial welding deformation and the center position of the annular seam by means of the cross laser and the spot laser cooperate with the vision sensor, and through the data analysis of the static and dynamic measurements, it can be seen that the measurement errors are all within the allowable range. However, the data of annular seam is difficult to be very accurate, due to the secondary welding. It is assumed that the wall thickness of the tube is uniform and the shape is regular. Therefore, the outer circumferential seam is calculated by measuring the inner circle of the tube and the fixed wall thickness. If the wall of the tube is deformation or incompleteness, it will result in a slight deviation in this measurement method. In the future, it will further improve the measurement accuracy of the center annular seam, if developed an accurate identification algorithm for outside of the tube (which is the true annular seam).

REFERENCES

- [1] S. Xu and W. Wang, "Numerical investigation on weld residual stresses in tube to tube sheet joint of a heat exchanger," *Int. J. Pressure Vessels Piping*, vol. 101, pp. 37–44, Jan. 2013.
- [2] R. Arias, E. Vaamonde, A. Vandewynckèle, E. Piñeiro, and P. Veron, "Laser welding of tube to tube-sheet joint in steam generators for nuclear power plants," in *Proc. 29th Int. Cong. Laser Mater. Process. Laser Microprocess. Nanomanuf.*, Anaheim, CA, USA, Sep. 2010, pp. 660–667.
- [3] A. Cobo, J. Mirapeix, F. Linares, J. A. Piney, D. Solana, and J. M. Lopez-Higuera, "Spectroscopic sensor system for quality assurance of the tube-to-tubesheet welding process in nuclear steam generators," *IEEE Sensors J.*, vol. 7, no. 9, pp. 1219–1224, Sep. 2007.
- [4] Z. Karastojkovic and Z. Janjusevic, "Welding methods of boiler tubes on lime deposit formation in power plant," *Weld. World*, vol. 49, no. 1, pp. 5–11, 2005.
- [5] L. N. Bagautdinova, R. S. Basyrov, I. I. Galimzyanov, A. F. Gaysin, A. F. Gaysin, F. M. Gaysin, and I. T. Fakhruddinova, "New technology for welding aluminum and its alloys," *Mater. Today: Proc.*, vol. 19, pp. 2566–2567, 2019.
- [6] T. Lei, "Research on position location and welding stability of robotic welding for large-scale tubesheet circular seam," Ph.D. dissertation, Huazhong Univ. Sci. Technol., Wuhan, China, 2021.

- [7] F. Dorsch, D. Pfitzner, and H. Braun, "Improved continuous tube welding due to unique process sensor system and process control," *Phys. Proc.*, vol. 41, pp. 137–139, Jan. 2013.
- [8] K. Suwanratchatamane, M. Matsumoto, and S. Hashimoto, "A novel tactile sensor torch system for robot manipulator and active object edge tracking," in *Proc. 34th Annu. Conf. IEEE Ind. Electron.*, Orlando, FL, USA, Nov. 2008, pp. 2617–2622.
- [9] Y. L. Xu, "Research on real-time tracking and control technology of three-dimension welding seam during welding robot GTAW process based on vision sensor and arc sensor," Ph.D. dissertation, Shanghai Jiao Tong Univ., Shanghai, China, 2013.
- [10] J. Pinto-Lopera, J. S. T. Motta, and S. Absi Alfaro, "Real-time measurement of width and height of weld beads in GMAW processes," *Sensors*, vol. 16, no. 9, p. 1500, Sep. 2016.
- [11] J. Muhammad, H. Altun, and E. Abo-Serie, "A robust butt welding seam finding technique for intelligent robotic welding system using active laser vision," *Int. J. Adv. Manuf. Technol.*, vol. 94, nos. 1–4, pp. 13–29, Jan. 2018.
- [12] S. B. Ario, "A study on automatic welding system of fixed aluminum pipes using vision sensors," Ph.D. dissertation, Keio Univ., Tokyo, Japan, 2009.
- [13] T. Lei, Y. Rong, H. Wang, Y. Huang, and M. Li, "A review of vision-aided robotic welding," *Comput. Ind.*, vol. 123, Dec. 2020, Art. no. 103326.
- [14] J. F. Fan, F. S. Jing, Z. J. Fang, and M. Tan, "Automatic recognition system of welding seam type based on SVM method," *Int. J. Adv. Manuf. Technol.*, vol. 92, no. 4, pp. 989–999, Sep. 2017.
- [15] X. Lü, D. Gu, Y. Wang, Y. Qu, C. Qin, and F. Huang, "Feature extraction of welding seam image based on laser vision," *IEEE Sensors J.*, vol. 18, no. 11, pp. 4715–4724, Jun. 2018.
- [16] T. Lei, W. Wang, Y. Rong, P. Xiong, and Y. Huang, "Cross-lines laser aided machine vision in tube-to-tubesheet welding for welding height control," *Opt. Laser Technol.*, vol. 121, Jan. 2020, Art. no. 105796.
- [17] L. Zhang, W. Ke, Q. Ye, and J. Jiao, "A novel laser vision sensor for weld line detection on wall-climbing robot," *Opt. Laser Technol.*, vol. 60, pp. 69–79, Aug. 2014.
- [18] L. Zhang, Q. Ye, W. Yang, and J. Jiao, "Weld line detection and tracking via spatial-temporal cascaded hidden Markov models and cross structured light," *IEEE Trans. Instrum. Meas.*, vol. 63, no. 4, pp. 742–753, Apr. 2013.
- [19] J. Guo, Z. Zhu, B. Sun, and Y. Yu, "Principle of an innovative visual sensor based on combined laser structured lights and its experimental verification," *Opt. Laser Technol.*, vol. 111, pp. 35–44, Apr. 2019.
- [20] P. Xu, X. Tang, R. Na, and S. Yao, "Study on welded seam recognition using circular laser vision sensor," *Chin Opt. Lett.*, vol. 5, no. 6, pp. 328–331, Jun. 2007.
- [21] J. Z. Wu, Z. J. Zhou, and Z. P. Liu, "The round hole alignment algorithm based on image recognition," *Mechatronics*, vol. 19, no. 1, pp. 18–21, Jan. 2013.
- [22] X. Zhang, "Vision-based research on position and path planning of tube sheet robot welding," M.S. thesis, Shandong Univ., Jinan, China, 2016.



XINGDONG WANG received the Ph.D. degree from the School of Mechanical Science and Engineering, Huazhong University of Science and Technology, Wuhan, China, in 2005. He is currently a Professor with the School of Machinery and Automation, Wuhan University of Science and Technology. His research interests include computer modeling and simulation of electromechanical systems, machine vision, and mechanical analysis of metallurgical machinery.



JIANYI KONG received the Ph.D. degree from Helmut-Schmidt-Universität, Hamburg, Germany. He is currently a Professor with the School of Machinery and Automation, Wuhan University of Science and Technology. His research interests include mechanism, mechanical and electronic engineering, and intelligent design and manufacturing.



YOUMIN RONG received the Ph.D. degree from the School of Mechanical Science and Engineering, Huazhong University of Science and Technology, Wuhan, China, in 2017. He is currently an Associate Professor with the Huazhong University of Science and Technology. His research interests include laser processing (welding, cutting) process mechanism, laser processing detection technology, and complete sets of equipment.



JIANHUA MA received the B.Sc. and M.Sc. degrees from the School of Mechanical Engineering and Mechanics, Xiangtan University, Xiangtan, China, in 2011 and 2014, respectively. He is currently pursuing the Ph.D. degree with the School of Machinery and Automation, Wuhan University of Science and Technology. His research interests include machine vision, automatic welding, and motion control.



YU HUANG received the Ph.D. degree from the School of Mechanical Science and Engineering, Huazhong University of Science and Technology, Wuhan, China, in 2004. He is currently a Professor and the Scholar of the Huazhong University of Science and Technology. His research interests include laser fine processing technology and equipment, high power laser processing technology and equipment, and high performance hydrostatic support technology and components.

...